Phase diagram of the CuO_3 chains in $YBa_2Cu_3O_{6+x}$ and $PrBa_2Cu_3O_{6+x}$

R. Franco[1] and A. A. Aligia[2]
[1]*Instituto de Física, Universidade Federal Fluminense (UFF), C.P 100.093, Avenida Litorânea s/n, 24210-340 Niterói, Rio de Janeiro, Brazil*
[2]*Comisión Nacional de Energía Atómica, Centro Atómico Bariloche and Instituto Balseiro, 8400 S.C. de Bariloche, Argentina*
(Received 29 December 2002; published 22 May 2003)

We use a mapping of the multiband Hubbard model for CuO_3 chains in $R\,Ba_2Cu_3O_{6+x}$ (R=Y or a rare earth) onto a t-J model and the description of the charge dynamics of the latter in terms of a spinless model, to study the electronic structure of the chains. We briefly review results for the optical conductivity and we calculate the quantum phase diagram of quarter filled chains including Coulomb repulsion up to that between next-nearest-neighbor Cu atoms V_2, using the resulting effective Hamiltonian, mapped onto an XXZ chain, and the method of crossing of excitation spectra. The method gives accurate results for the boundaries of the metallic phase in this case. The inclusion of V_2 greatly enhances the region of metallic behavior of the chains.

DOI: 10.1103/PhysRevB.67.172507 PACS number(s): 74.72.Bk, 71.30.+h, 75.10.Jm

There is consensus in that the electronic structure of $R\,Ba_2Cu_3O_{6+x}$ (R=Y or a rare earth) can be separated into that of the two CuO_2 planes per unit cell which become superconducting under doping, and that of the CuO_{2+x} subsystem, in which CuO_3 chains are formed for oxygen content $x \geqslant 0.5$ and low temperatures.[1] The electronic structure of the CuO_3 chains is crucial because it controls the doping of the superconducting CuO_2 planes. The dependence of the superconducting critical temperature T_c with annealing,[2] combined with Raman measurements[3] and persistent photoconductivity experiments,[4,5] show an intimate relation between the oxygen ordering in the CuO_x planes and T_c:[6] oxygen ordering along chains increases the amount of twofold and fourfold coordinated Cu atoms at the expense of threefold coordinated ones, and leads to an increase in the hole doping of the superconducting CuO_2 planes. Detailed calculations of the relation between electronic and atomic structure in $R\,Ba_2Cu_3O_{6+x}$, together with a simple explanation of the above facts valid in the strong-coupling limit were presented.[1] These results show the relevance of interatomic Coulomb interactions. In addition even near the optimum doping ($\sim$1/5 holes per Cu atom in the planes), the average distance between carriers is of the order of two lattice parameters of the planes suggesting that interatomic repulsion at smaller distances are screened only partially.

Several pieces of evidence suggest that the CuO_3 chains are insulating. For example, $PrBa_2Cu_3O_7$ is semiconducting,[7] and the contribution of the CuO_3 chains to the optical conductivity $\sigma(\omega)$ is very similar in this compound[8] and in superconducting $YBa_2Cu_3O_{6+x}$,[9,10] displaying a broad peak near $\omega \sim 0.2$ eV and a slowly falling tail at higher frequencies. Also, charge modulations observed by scanning tunneling microscopy (STM) were interpreted in terms of a charge-density wave and a gap in the spectrum of the chains.[11] Finally, in the explanation of Fehrenbacher and Rice of the suppression of superconductivity upon substituting Y by Pr in $YBa_2Cu_3O_7$, they propose that the holes which dope the superconducting CuO_2 planes in $YBa_2Cu_3O_7$ are displaced towards a hybrid Pr-O state in $PrBa_2Cu_3O_7$.[12] This implies a shift in the Fermi level of about 0.25 eV according to their parameters, while the authors *assume* that the hole occupation of the CuO_3 chains is 0.5 in both cases. Thus this explanation seems to require a gap in the chains to be consistent.

However, all he above data can also be consistently explained assuming intrinsically *metallic* chains cut by $\sim$5% of defects or oxygen vacancies ($x \sim 0.95$), which is usual in these systems.[13] The appropriate multiband model for CuO_3 chains was mapped numerically into a t-J model with $t \sim 0.85$ eV and $J \sim 0.2$ eV. With these parameters, the decrease in the occupation of the chains upon replacing Y by Pr is only 0.05. Taking into account that the charge dynamics of the model can be described up to a few percent by a spinless model even for $J/t=0.4$,[13,14] charge modulations and the optical conductivity can be explained.[13] In particular, the lower energy part of the latter is given by

$$\sigma(\omega) = \frac{AB}{\omega^2} \exp(-A/\omega), \tag{1}$$

with

$$A = -2t\pi \ln(1-c)\sin k_F; \quad B = \frac{e^2}{\hbar}(1-c^2)t \sin k_F,$$

and $c=1-x$ is the concentration of oxygen vacancies . The experimental results were fitted using $A=0.35$ eV.[13] The resulting optical conductivity below 0.4 eV is shown in Fig. 1. Note that in spite of the metallic character of the chains, as a consequence of the oxygen defects, $\sigma(\omega)$ has a pseudogap at low energies. The experiments cannot confirm this due to large errors for $\omega < 0.1$ eV.[8–10] However, recent STM studies of the local density of states detect a pseudogap of about 25 meV and numerous intragap resonances.[15] The latter might be explained by the effect of defects on superconductivity in the chains induced by proximity,[16] but also in principle by eigenstates of long finite metallic chains. Unfortunately, the local density of states of the one-dimensional t-J model depends also on the spin-wave function and cannot be described solely by spinless fermions.[17,18]

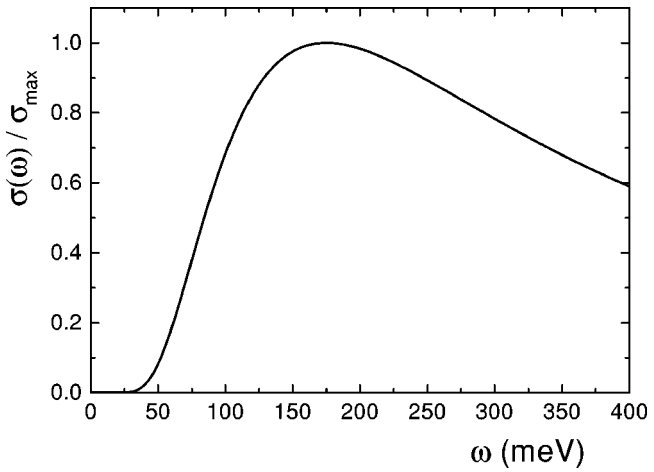

FIG. 1. Low-energy part of the optical conductivity of CuO_3 chains for $A=0.35$ eV [see Eq. (1)].

The natural candidate to open a gap in the effective t-J model for the CuO_3 chains is the nearest-neighbor repulsion V_1. Keeping the assumption that the charge dynamics is described by a spinless model, one expects that a gap opens for $V_1>2t\sim 1.7$ eV.[19,20] If the Coulomb repulsions were completely unscreened $V_1\sim e^2/b\cong 3.6$ eV, where b is the lattice parameter along the chains. Recently Seo and Ogata showed that inclusion of next-nearest-neighbor repulsion V_2 enhances the range of stability of the metallic phase, calculating the gap as a function of V_2.[21]

We calculate the phase diagram of the spinless model, including V_1 and V_2 using the method of crossing of excitation levels.[22–24] Actually, the mapping of the energy of the one-dimensional t-J model into that of a spinless model is strictly valid only for $J=0$,[17,20,21] but we expect it to be a very good approximation for $J/t<0.4$.[13,14] The advantage of the method of level crossings, briefly explained below, over previous approaches[21,25] is the accuracy that can be achieved for the phase boundaries. This has been shown for example in its application to the Hubbard model with correlated hopping[26,27] in comparison with exact results.[28]

In standard notation, the model is

$$H=\sum_i \left[t(c_{i+1}^{\dagger}c_i+\text{H.c.})+V_1 n_i n_{i+1}+V_2 n_i n_{i+2}\right], \quad (2)$$

with $n_j=c_j^{\dagger}c_j$. Using a Jordan-Wigner transformation $S_j^+=c_j^{\dagger}\exp(i\pi\Sigma_{l<j}n_l)$, $S_j^-=(S_j^+)^{\dagger}$, $S_j^z=n_j-1$, the model can be mapped into an XXZ model with next-nearest-neighbor antiferromagnetic Ising interaction,

$$H=\sum_i \left[J_1(S_i^x S_{i+1}^x+S_i^y S_{i+1}^y)+\Delta_1 S_i^z S_{i+1}^z+\Delta_2 S_i^z S_{i+2}^z\right], \quad (3)$$

where S_i^{β} is the β component of the spin-1/2 operator at site i, $J_1=2t$, and $\Delta_j=V_j$.[20,21]

A successful approach to describe the qualitative properties of one-dimensional strongly correlated systems is bosonization followed by a renormalization-group procedure. This procedure usually terminates at a fixed point, which determines the properties of the system for the initial parameters given. A phase transition occurs when the flow goes towards a different fixed point. Since the renormalization group is a weak-coupling approach, the phase boundaries are not given accurately by the method for large interactions. The basic idea of the method of level crossings is to combine numerical calculations of excitation levels with basic knowledge on the properties of these fixed points. The more interesting phase transitions involve one fixed point which is scale invariant. This is for example the case of the XXZ model with next-nearest-neighbor interactions studied by Nomura and Okamoto.[22] The spin fluid phase of Eq. (3) [which corresponds to the metallic phase of Eq. (2)], like that of an ordinary Heisenberg model is characterized by a scale invariant fixed point.[22] Then, using conformal field theory one can relate the excitation energy which corresponds to some operator A_i at site i (for example a spin flip S_i^+, S_i^-), to the dependence of the correlation functions of this operator with distance d, for large d:

$$E_A(L)-E_g(L)=\frac{2\pi v x_A}{L}, \langle A_{i+d}A_i\rangle\sim\frac{1}{d^{2x_A}}. \quad (4)$$

Here L is the length of the system, v the spin-wave velocity, $E_g(L)$ the ground-state energy, $E_A(L)$ the lowest energy in the adequate symmetry sector (connected to the ground state by A_i) and x_A the critical dimension for the excitation A. Since the dominant correlations at large distances determine the nature of the thermodynamic phase, a phase transition is determined by the crossing of excited levels for different symmetry sectors.

TABLE I. Quantum numbers of the ground state and the first excited state of the different phases for L multiple of four.

	K	S^z	P	T
Ground state	0	0	1	1
Exc. spin fluid	π	± 1	-1	-
Exc. AFI	π	0	-1	-1
Exc. dimer, AFII	π	0	1	1

In the present problem, the relevant quantum numbers which determine the symmetry sector are total wave vector K, total spin projection S^z, parity under inversion P and parity under time reversal T. We have restricted our calculations to number of sites L multiple of four to avoid frustration of the phase which we call AFII (see below). For these sizes, the quantum numbers of the ground state are always the same in the region of parameters studied. They are listed in Table I, together with the quantum numbers of the first excited state of each phase. Our main interest are the boundaries of the spin fluid phase of the spin model Eq. (3) which corresponds to the metallic phase of Eq. (2). With increasing Δ_1 (Δ_2) there is a continuous transition to an insulating Néel ordered (dimerized) phase.[22] The Néel ordered phase, which we call antiferromagnetic I (AFI) for maximum order parameter has a spin ordering $\uparrow\downarrow\uparrow\downarrow\cdots$ and corresponds to a

charge ordering $1010\cdots$ in the original model Eq. (2). The dimer phase has a gap which is exponentially small near the metallic phase.[22] This renders it very difficult to detect the transition with alternative numerical methods.[27] The transitions between any two of these three phases were determined accurately from the corresponding crossing of excited levels (see Table I). In addition, with increasing Δ_2, we expect a transition from the dimer phase to an AFII a phase with long-range order $\uparrow\uparrow\downarrow\downarrow\cdots$ (corresponding to charge ordering $1100\cdots$). This transition cannot be detected by crossing of first excited states. Since it involves two insulating phases, it is not described by a scale invariant theory and is also beyond our scope. For the sake of completeness we have drawn a tentative dimer-AFII boundary using the rough criterium that the system is in the AFII phase when the ground-state correlation function (calculated deriving the energy using Hellmann-Feynman theorem) $\langle S_i^z S_{i+2}^z\rangle < -1/8$. For the other transitions, we have calculated the transition points in systems with $L=12$, 16, and 20 sites. According to field theory predictions for large enough L, these points plotted as a function of $1/L^2$ should lie on a straight line.[22,29] We have verified that this is the case for the three transitions with high accuracy. The linear fit provided the transition point extrapolated to $1/L^2 \to 0$, and is error. The error is below 1% in all cases, confirming the validity of the method in the present case.

The resulting phase diagram is shown in Fig. 2. For $V_2 = \Delta_2 = 0$, the known exact results[19,20] are reproduced: there is a transition from the spin fluid (metallic) phase to the AFI (charge density wave) phase at $\Delta_1 = J_1$ ($V_1 = 2t$). Another known limit is the classical one $J_1 \to 0$ ($t \to 0$), for which there is a transition between both AF phases at $\Delta_2 = \Delta_1/2$ ($V_2 = V_1/2$). Our results are consistent with this limit. However, there is a strip of width $\sim J_1 = 2t$ of a dimer phase between both AF (charge ordered insulating) phases. This is reminiscent of the physics of the ionic Hubbard model, for which a strip of a dimer phase of width $\sim 0.6t$ in the strong-coupling limit separates the band insulating and the Mott insulating phases[24] dye to the charge fluctuations that still remain in the strong-coupling limit.

In qualitative agreement with previous calculations,[21] we obtain that the addition of V_2 greatly enhances the range of stability of the metallic phase of the CuO_3 chains in

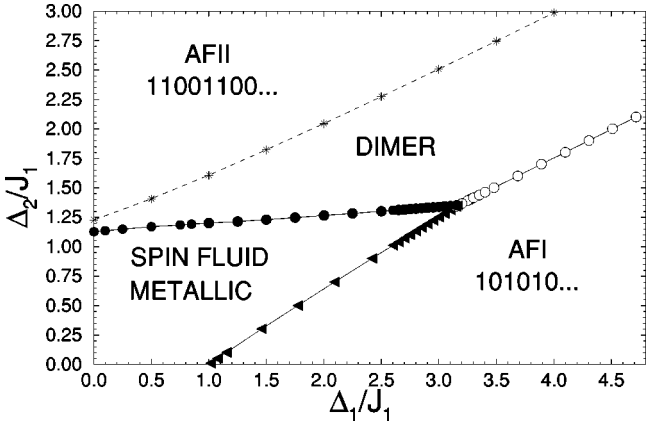

FIG. 2. Phase diagram of the effective model for CuO_3 chains [Eqs. (2) or (3)] as a function of $\Delta_1/J_1 = V_1/2t$ and $\Delta_2/J_1 = V_2/2t$.

$R\,Ba_2Cu_3O_{6+x}$. For unscreened interactions $V_1 = 2V_2 \cong 3.6$ eV. Using $J_1 = 2t = 1.7$ eV, one can see from the phase diagram that the system falls in the metallic phase even in this extreme case. Instead, if V_2 were neglected the chains would be in an insulating charge ordered state for the same t and V_1.

A numerical mapping of the appropriate multiband Hubbard model for the chains to a t-J model indicates that $J/t < 1/4$.[13] It is reasonable to expect that turning J to zero does not change sustantially the phase diagram. For $J=0$, the mapping from the generalizaed t-J model to the spinless model is exact and our results lead to the conclusion that the CuO_3 chains in $R\,Ba_2Cu_3O_{6+x}$ (R=Y or a rare earth) are intrinsically metallic. Observed charge modulations are likely due to Friedel oscillations induced by defects, like O vacancies. These defects or superconductivity induced by the CuO_2 planes can also lead to the observed pseudogap behavior.

This work was sponsored by PICT's 03-06343 of ANPCyT, Argentina. R. Franco is grateful to the National Research Council (CNPq), Brazil, by their financial support. A. A. Aligia was partially supported by CONICET, Argentina.

[1] A. A. Aligia and J. Garces, Phys. Rev. B **49**, 524 (1994), and references therein.
[2] B. W. Veal, A. P. Paulikas, Hoydoo You, Hao Shi, Y. Fang, and J. W. Downey, Phys. Rev. B **42**, 6305 (1990).
[3] J. Kircher, E. Brücher, E. Schönherr, R. K. Kremer, and M. Cardona, Phys. Rev. B **46**, 588 (1992).
[4] V. I. Kudinov, I. L. Chaplygin, A. I. Kirilyuk, N. M. Kreines, R. Laiho, and E. Lähderanta, Phys. Lett. A **157**, 290 (1991).
[5] G. Nieva, E. Osquiguil, J. Guimpel, M. Maenhoudt, B. Wuyts, Y. Bruynseraede, M. B. Maple, and I. K. Schuller, Phys. Rev. B **46**, 14 249 (1992).
[6] A. A. Aligia, Phys. Rev. Lett. **73**, 1561 (1994).
[7] L. Soderholm, K. Zhang, D. G. Hinks, M. A. Beno, J. D. Jorgensen, C. U. Segre, and I. K. Shuller, Nature (London) **328**, 604 (1987).
[8] K. Takenaka, Y. Imanaka, K. Tamasaku, T. Ito, and S. Uchida, Phys. Rev. B **46**, 5833 (1992).
[9] Z. Schlesinger, R. T. Collins, F. Holtzberg, C. Field, S. H. Blanton, U. Welp, G. W. Crabtree, Y. Fang, and J. Z. Liu, Phys. Rev. Lett. **65**, 801 (1990).
[10] L. D. Rotter, Z. Schlesinger, R. T. Collins, F. Holtzberg, C. Field, U. W. Welp, G. W. Crabtree, J. Z. Liu, Y. Fang, K. G. Vandervoort, and S. Fleshler, Phys. Rev. Lett. **67**, 2741 (1991).
[11] H. L. Edwards, A. L. Barr, J. T. Markert, and A. L. deLozanne Phys. Rev. Lett. **73**, 1154 (1994).

[12] R. Fehrenbacher and T. M. Rice, Phys. Rev. Lett. **70**, 3471 (1993).
[13] A. A. Aligia, E. R. Gagliano, and P. Vairus, Phys. Rev. B **52**, 13601 (1995).
[14] T. Tohyama, P. Horsch, and S. Maekawa, Phys. Rev. Lett. **74**, 980 (1994).
[15] D. J. Derro, E. W. Hudson, K. M. Lang, S. H. Pan, J. C. Davis, J. T. Markert, and A. L. deLozanne, Phys. Rev. Lett. **88**, 097002 (2002).
[16] D. K. Morr and A. V. Balatsky, Phys. Rev. Lett. **87**, 247002 (2001).
[17] K. Penc, K. Hallberg, F. Mila, and H. Shiba, Phys. Rev. B **55**, 15475 (1997).
[18] C. Kim, P. J. White, Z.-X. Shen, T. Tohyama, Y. Shibata, S. Maekawa, B. O. Wells, Y. J. Kim, R. J. Birgeneau, and M. A. Kastner, Phys. Rev. Lett. **80**, 4245 (1998).
[19] J. D. Johnson, S. Krinsky, and B. M. Mc Coy, Phys. Rev. A **8**, 2526 (1973).
[20] A. A. Aligia and G. Ortiz, Phys. Rev. Lett. **82**, 2560 (1999).
[21] H. Seo and M. Ogata, Phys. Rev. B **64**, 113103 (2001).
[22] K. Nomura and K. Okamoto, J. Phys. A **27**, 5773 (1994).
[23] M. Nakamura, Phys. Rev. B **61**, 16377 (2000).
[24] M. E. Torio, A. A. Aligia, and H. A. Ceccatto, Phys. Rev. B **64**, 121105(R) (2001).
[25] A. K. Zhuravlev, M. I. Katsnelson, and A. V. Trefilov, Phys. Rev. B **56**, 12 939 (1997); A. K. Zhuravlev and M. I. Katsnelson, *ibid.* **61**, 15534 (2000).
[26] A. A. Aligia and L. Arrachea, Phys. Rev. B **60**, 15 332 (1999). There is a misprint in Eq. (11) which should read $g_\rho = g_{1\|} - 2g_{2\|} - 2g_{2\perp}$, $g_\sigma = g_{1\|} - 2g_{2\|} + 2g_{2\perp}$.
[27] A. A. Aligia, K. Hallberg, C. D. Batista, and G. Ortiz, Phys. Rev. B **61**, 7883 (2000).
[28] L. Arrachea, A. A. Aligia, and E. Gagliano, Phys. Rev. Lett. **76**, 4396 (1996), and references therein.
[29] Actually, the $1/L^2$ scaling is not expected to work for the transition between gapped phases, like AFI and dimer, unless the gap is very small at the transition.